American Mineralogist, Volume 67, pages 1195–1205, 1982

Electron microscopy of a muscovite–biotite interface

SUMIO IIJIMA[1] AND JING ZHU[2]

Center for Solid State Science
Arizona State University
Tempe, Arizona 85281

Abstract

An intergrowth of mucovite and biotite from Mitchell Creek Mine, Upson County, Georgia, was studied with a high resolution transmission electron microscope. Atomic arrangements of the interface between muscovite and biotite have been derived, revealing far more complexity for the interface structure than that proposed previously based on optical and X-ray analysis (Gresens and Stensrud, 1971).

It was found that the muscovite has an almost perfectly ordered $2M_1$ structure, while the biotite is highly disordered. Despite such disorder in biotite, both octahedral layers and K ion interlayers of the two minerals are connected perfectly at the interface, while about 60% of the tetrahedral sheets are discontinued across the interface.

Occasional occurrences of coherent intergrowths of chlorite-like structure in biotite were recognized in the vicinity of the interface.

Introduction

Interface structures between two minerals, which result from precipitation or exsolution involving diffusion of particular atoms in the system, have been studied to determine their crystallization histories (see, for example, Wenk, 1976; Veblen and Buseck, 1981). Atomic structures or morphology of such boundaries are influenced by thermal history and evolution of the minerals. The configuration energy of the interfaces, for which misfit dislocations or other types of lattice relaxation may be present, tends to be minimized. Therefore, elucidation of the atomic structures of interfaces is important in the study of minerals.

The specimen of intergrown crystals of muscovite and biotite examined in the present study is from the Mitchell Creek Mine, Upson County, Georgia (pegmatite). In this single mica book a pyramidal crystal of biotite has intergrown in muscovite. The same crystal has been studied formerly by Gresens and Stensrud (1971), and its detailed description has been given in their paper and also by Lester (1946). Under the optical microscope, the interfaces are not always sharp and straight in the (001) plane projection. The book containing the two micas can be cleaved easily through the interface without breaking it, suggesting a good continuity of the two minerals across the interface. The book contains small inclusions of other minerals near the biotite, such as pyrite and apatite.

From the optical properties and the X-ray diffraction pattern of this intergrowth, Gresens and Stensrud (1971) proposed that the basic tetrahedral sheets of the micas continue across the interface between the two minerals. They also suspected that a slight difference in the d_{001} values between the two minerals might be accommodated by edge dislocations formed parallel to (001) planes. In the present study, we used the high resolution transmission electron microscopy technique to investigate atomic structures of the interface between the muscovite and biotite. The technique provides more information on the interface structures that has been previously obtained (Gresens and Stensrud, 1971).

Technique

Useful information on the interface between the two micas can be obtained by examining its cross section in a direction parallel to the layers. Edges of the biotite intergrown in muscovite are parallel to the ⟨100⟩ or ⟨110⟩ directions of $2M_1$ muscovite. In projections along those directions of the crystal,

[1]Present address: Research and Development Corporation of Japan, Department of Physics, Meijo University, Yagoto-Urayama Tepaku-ku, Nagoya, Japan.

[2]On leave from Central Iron and Steel Research Institute, Beijing, People's Republic of China.

0003–004X/82/1112–1195$02.00

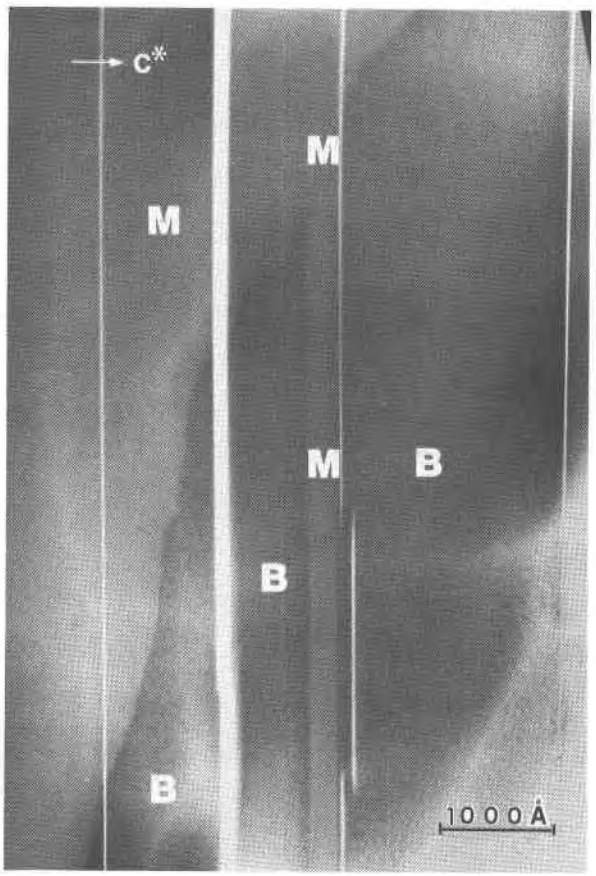

Fig. 1. Low magnification electron micrograph of an interface between biotite (B) and muscovite (M). The crystal is oriented with [110] parallel to the electron beam. Note that a slab of muscovite having a width of 300Å penetrates into biotite.

positions of the alkali ions in the interlayers are seen on end. When going from one layer to the next, these positions can be utilized for describing a stacking sequence of the mica layers, as reported previously (Iijima and Buseck, 1978).

The method for the preparation of the specimen by sectioning a mica crystal with a diamond knife in an ultramicrotome (Iijima and Buseck, 1978) is not suitable for the present purpose and thus the specimen was prepared by an ordinary ion beam thinning method. However, the easy cleavage of mica crystals and the necessity of pin-pointing an interface in the crystal required very careful specimen preparation.

A thin specimen was prepared by argon ion milling, in which great care was taken not to completely erode the interface region. The specimen was lightly carbon coated. A JEOL 200CX transmission electron microscope operated at 200 kV and equipped with a top-entry goniometer stage was used. The tilting specimen cartridge accepting a standard specimen of 3 mm diameter was built in our laboratory.

Results and interpretation

Morphology of the interface

Lester (1946) noted that in the thick book of mica examined presently the biotite is intergrown in muscovite as pyramidal shapes. Gresens and Stensrud (1971), however, found that the contact of the two minerals has occasional irregularities, and small, irregular patches of biotite were recognized in the muscovite. They also speculated that similar small patches of muscovite might occur in biotite. These observations suggest inhomogeneous distribution of (Fe, Mg) ions and Al ions near the interface.

A low magnification electron micrograph (Fig. 1) of an interface from our sample provides a view of the overall microscopic morphology of the interface and immediately answers some of the questions raised from the light microscope examination.

A curving line running approximately from the top right to the bottom left partitions two regions, the dark region which is biotite and the lighter one which is muscovite. This was confirmed by examining peak heights of Fe in the X-ray energy dispersive spectra from these two regions. The measurement was conducted with a Philips 400T microscope equipped with a Tracor Northern TN2000 EDS spectrometer. The darker contrast in biotite than in muscovite is attributed to the Fe ions, since they have a higher scattering cross section for the electrons than the Al ions in muscovite. The crystal was oriented so that the $[\bar{1}\bar{1}0]$ or $[1\bar{1}0]$ direction of the $2M_1$ of muscovite was parallel to the direction of the incident electron beam. An electron diffraction pattern from the muscovite is shown in Figure 2a.

Vertical white lines in Figure 1 are images of gaps in the crystal due to the cleavage introduced during the sample preparation. It is noted that a narrow band of muscovite about 300Å wide penetrates into a region of biotite (marked M in the middle of the photograph). We could not confirm whether or not the band is terminated in biotite. As we describe later, two types of interface between muscovite and biotite can be characterized, one parallel to the mica layers and one perpendicular to the layers. The boundary inclined to the layers can be considered as a mixture of these two types. The penetrat-

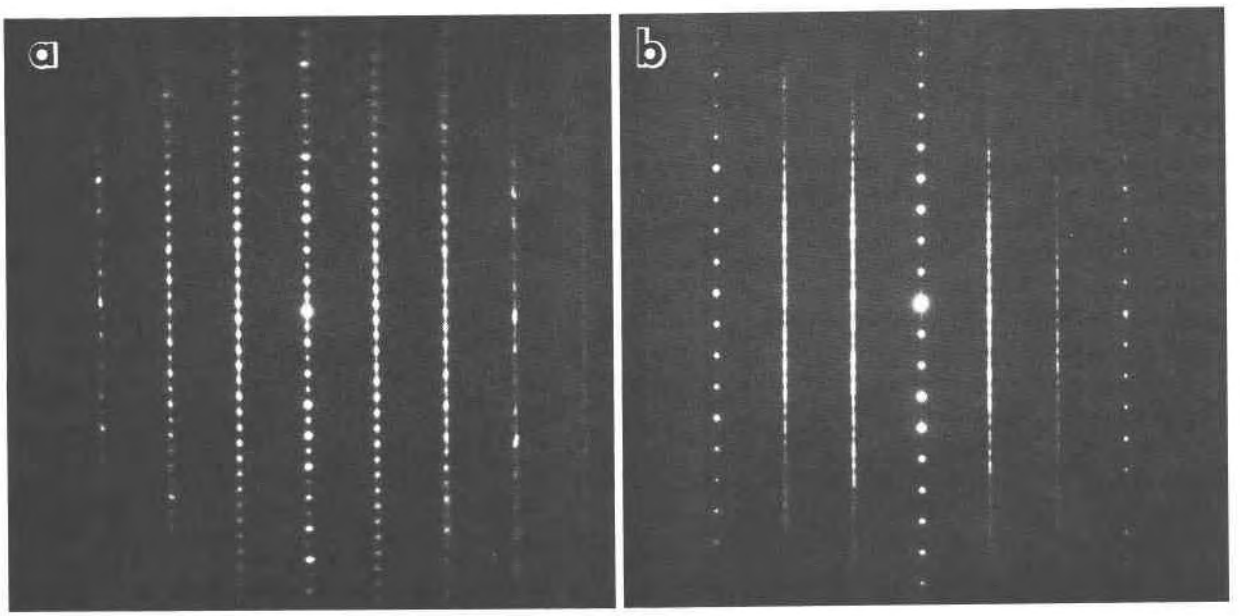

Fig. 2. A pair of electron diffraction patterns, (a) from a region of muscovite and (b) from a region of biotite, which lie next to each other at the interface. The muscovite shows sharp spots of the ($3k$ k l) reciprocal lattice section, while the biotite shows diffuse streaking at the spots with $k \neq 3n$.

ing slab of muscovite has an interface perfectly parallel to the mica layers as seen in Figure 1.

Figure 3 shows a low magnification image of another portion of the interface. The dark portion is biotite, an electron diffraction pattern (Fig. 2b) from which displays diffuse streaks at the reciprocal lattice points with $k \neq 3n$. The origin of the diffuse streaks has been explained by the occurrence of random 120n° layer rotations. The disordered stacking of the layers can be recognized in the image of biotite (Fig. 3), while the muscovite is almost perfectly ordered as demonstrated by the sharp diffraction spots in Figure 2a.

Atomic structure of the perpendicular interface

The dark contrast appearing along the interface could be caused by dislocations formed by discontinuities of the mica layers at the interface. A high resolution two-dimensional lattice image of the interface corresponding to the small area enclosed in Figure 3 is shown in Figure 4a. The crystal was not sufficiently thin and its orientation was not aligned precisely enough at the zone axis orientation, so that the image intensity of this image can not be interpreted directly in terms of the projection of the structure.

However, it was demonstrated in our previous study on disordered micas that two-dimensional lattice images viewed along the ⟨100⟩ or ⟨110⟩ directions are adequate to derive a stacking sequence of the layers (Iijima and Buseck, 1978). It was experimentally shown that in any one image the same portion of every unit cell of a perfect crystal always produces an identical image intensity, which is independent of the crystal diffraction parameters and the instrumental parameters. This is due to the fact that the spread of the electron wave traveling through the crystal is confined within a small area of several ångströms depending on the crystal thickness. The usefulness of such high resolution lattice images was demonstrated recently by the structure analysis of the sheet silicate mineral mcGillite by one of the present authors (Iijima, 1982a,b).

Let us consider the image details of the region of muscovite marked M in Figure 4a. The image shows three different intensity distributions for individual slabs having a 10Å width, which matches the spacing of the basic mica layer. They correspond to the three different projections of the basic mica layer along the [100], [110], and [1$\bar{1}$0] directions. The position symbols, A, B, and C, designated by Zvyagin (1962), can be used to describe the stacking sequence of the layers. We assume that in the present mica crystal there is no stacking disorder

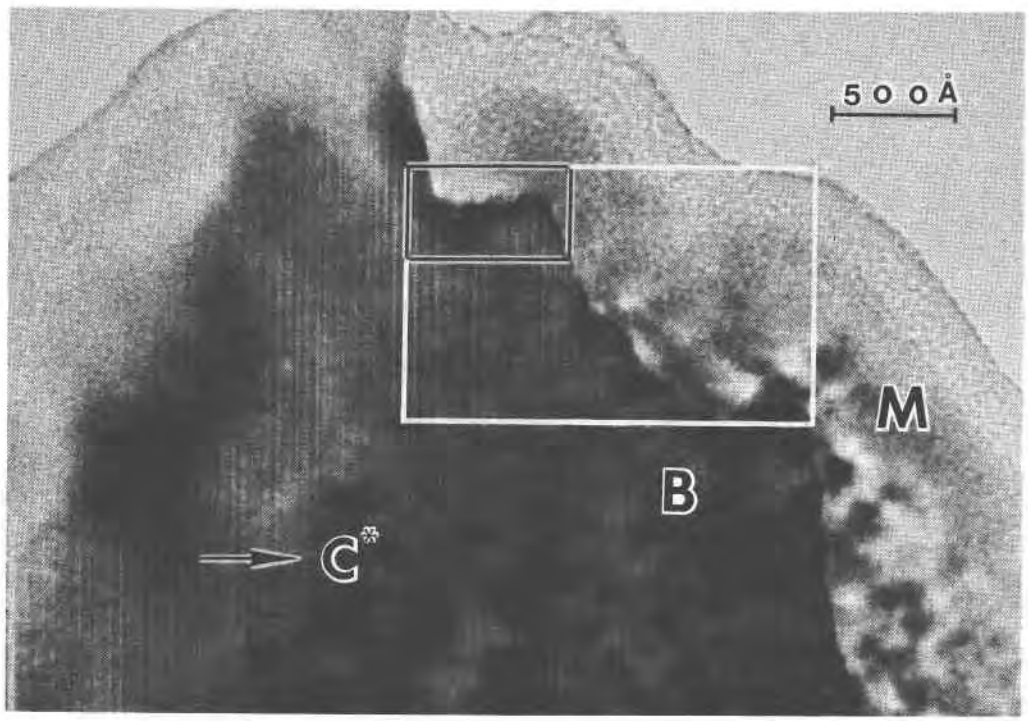

Fig. 3. A low magnification electron micrograph showing an interface between biotite (B) and muscovite (M). The dark contrast appearing along the boundary may be caused by lattice strain. The regions enclosed by the small and large rectangles are shown in Figs. 4 and 8 respectively.

due to 60°, 180°, or 300° rotations of the layers, which are uncommon in muscovite and biotite (Ross *et al.*, 1966).

Using these symbols we obtained the stacking sequence shown at the top of Figure 4a. Similarly, the stacking sequence labelled in Figure 4a is illustrated in Figure 5a by using the vector symbols of Smith and Yoder (1956). These vectors define the slip direction from the bottom tetrahedral sheet to the top one of the T–O–T layer projected on the (001) plane. The sequential numbers shown on the vectors correspond to layer numbers between 1 and 36.

These illustrations demonstrate that the crystal has the two-layer periodicity –BC– of the $2M_1$ structure, viewed down the [110] direction. This agrees with the electron diffraction pattern of Figure 2a. However, there are occasional stacking faults, as indicated by –CA– at the layer number 4–5, –AC– at the layer number 15–16, and –CAC– at the numbers 22–24.

Similarly, a stacking sequence in the region of biotite marked B in Figure 4a was analyzed. The result is shown at the bottom of the image, and the vector representation of the sequence is given in Figure 5b. As expected from the electron diffraction pattern (Fig. 2b), the stacking sequence is almost random, except for the region corresponding to the numbers 26–32. This region has the same –BC– stacking sequence as the muscovite, and the layers appear to be continuous across the interface. Disorder of the stacking can be seen best by viewing the micrograph at a grazing angle in the direction perpendicular to the layers.

Lattice fringes with 10Å spacing corresponding to a single layer appear to be continuous across the interface. This suggests that individual T–O–T mica layers and the K ion interlayers are registered perfectly in their z axis coordinates on both sides of the interface. This may be the reason why the mica book cleaves smoothly through the interface. However, it should be emphasized that the periodic stacking of the layers in muscovite becomes abruptly disordered in crossing the interface into biotite. The spatial transformation from biotite to muscovite takes place within a range of several unit cells at the interface.

Figure 4b represents a dark field electron micrograph of the same area of biotite as shown in Figure 4a. This was imaged using only the (00l) reflections

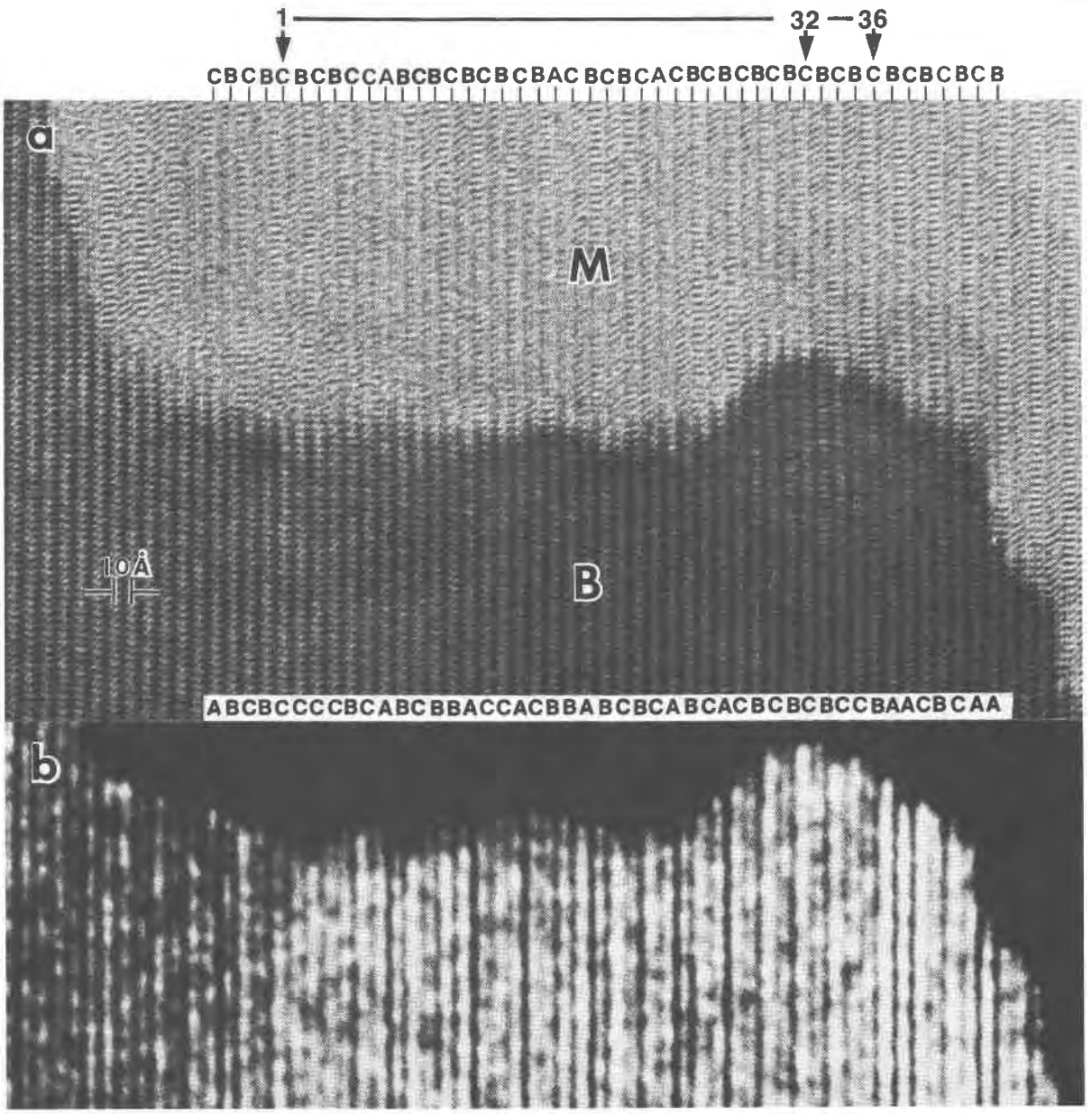

Fig. 4. (a) A high resolution lattice image of the region enclosed by the small rectangle in Fig. 3. The capital letters indicate the stacking layer sequences represented by Zvyagin's position symbols obtained by the analysis of the image intensity. The muscovite has a nearly ordered stacking sequence –BC– corresponding to the $2M_1$ polymorph, while the biotite is almost completely disordered. Continuities of the individual layers from layer numbers 1 to 36 have been analyzed in the text. (b) A dark field electron micrograph of the same region as for the bright field image of (a), showing variations in contrast which are consistent with the stacking sequence obtained from (a).

with $l = 1,2,3$. It is seen that the fringe images consist of lines having three different contrast levels; namely, the darkest, dark and grey lines. If the darkest line appears at the layer position A, the positions of the darkest lines match well with the layers A which were determined from Figure 4a. Similarly, the correspondence of the dark and grey lines to the layers B and C respectively is excellent. The dark field image therefore supports our interpretation of the stacking sequence in biotite derived from the bright field image. The region of muscovite has been vitrified entirely due to electron beam

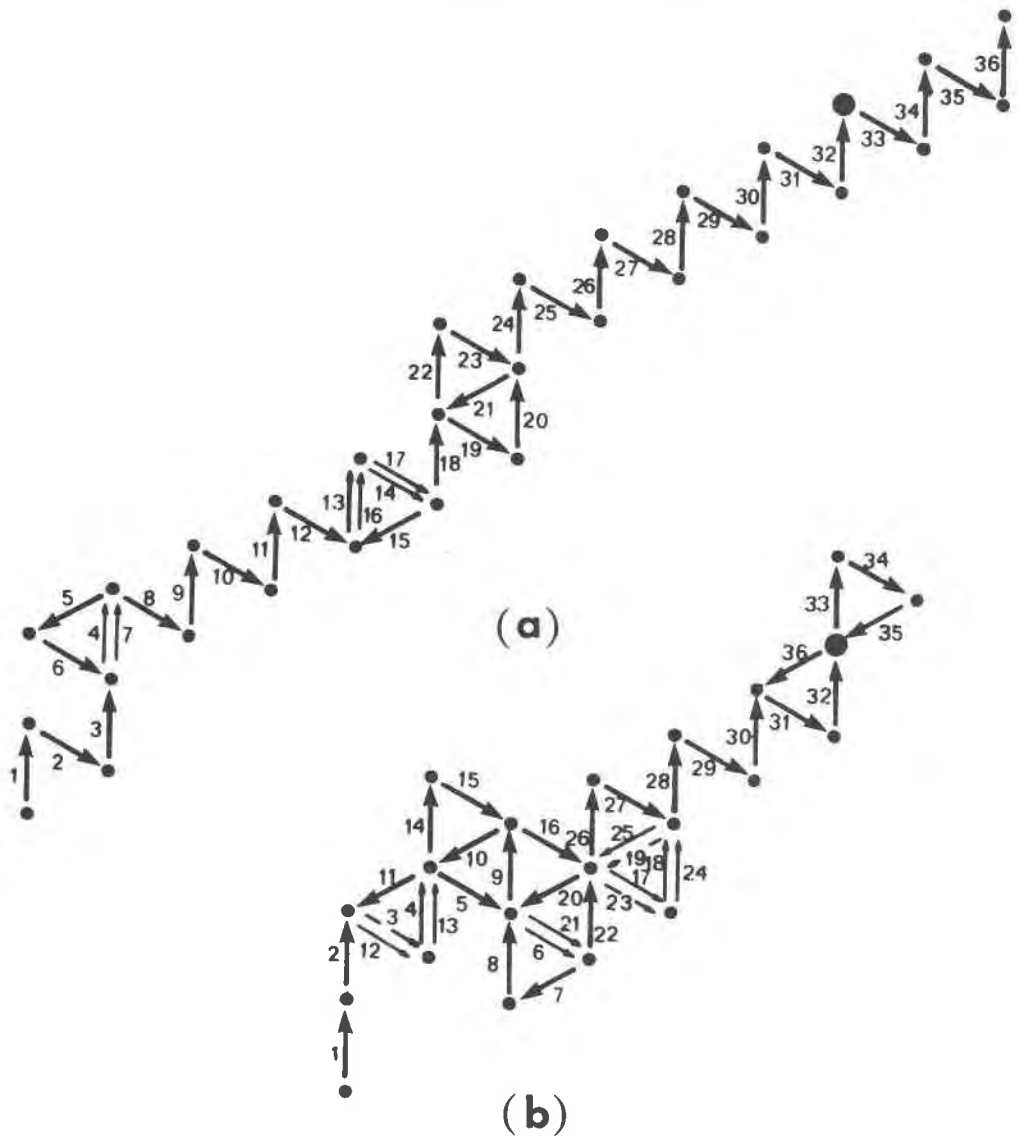

Fig. 5. Vector representations of the stacking layer sequences; (a) muscovite of Figure 4a and (b) biotite. The numbers on the vectors are the layer numbers. Note that the layers from numbers 26 to 32 are perfectly continuous across the interface.

damage, while the damage to the biotite is much less. A further point concerning this observation will be discussed later.

Now we consider atomic arrangements of the interface from the experimental results mentioned above. The Zvyagin position symbols define the relative positions of neighboring layers and are inconvenient for comparing two layers at the same level, as for discontinuous tetrahedral sheets. For instance, the C layer of the layer number 4 in muscovite in Figure 4a does not necessarily connect perfectly to the C layer of the layer number 4 of biotite, and the type of connection will be dependent on their adjacent layers. For this reason, the vector representation symbols were used for analysis of the atomic structure of the interface.

As described above, the individual layers of mica between the layer numbers 26 and 32 appear to be perfectly continuous across the interface. We take one of these layers, namely number 32, as a reference to the others. In other words, the two stacking vectors of number 32 shown in Figure 5a and 5b are superimposed. By doing so, we can find the positions of the individual T–O–T layers of the musco-

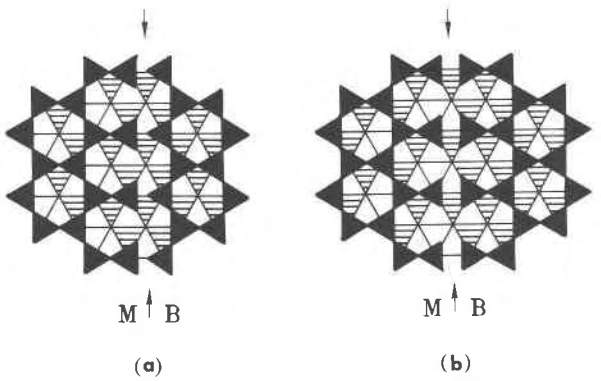

Fig. 6. Two possible idealized models for discontinued tetrahedral sheets at the interface (arrowed) between muscovite (M) and biotite (B), which were obtained by the analysis of the stacking vectors in Fig. 5. Dark and hatched triangles represent Si–O tetrahedra pointing down and octahedra in the T–O–T layer respectively. The arrangement shown in (a) seems to be favored over the one in (b).

vite relative to those of the biotite. Thus, we can examine the continuity of the individual T–O–T layers.

The analysis of the vectors showed that there are only two possible atom arrangements for the discontinuous layers, assuming a perfectly sharp interface. They are schematically illustrated in Figures 6a and 6b, where solid triangles represent the Si–O tetrahedral layers pointing down and hatched triangles the Al–O or Fe–O octahedral layers. In muscovite the octahedral layers contain Al ion vacancies. M and B indicate muscovite and biotite. We found that among the 49 T–O–T layers labelled in Figure 3a, 37% of them were continuous. Another 37% of layers are discontinuous and have the structure of Figure 5a. The rest of the layers are also discontinuous, with the structure of Figure 5b.

Because the actual T–O–T layers contain two tetrahedral sheets, each of which has one of the three structures described above, there are six possible structures for a T–O–T layer. The most common combination among the layers labelled in Figure 4a was such that one tetrahedral sheet is continuous and the other is that of Figure 6a. The least common one is such that both top and bottom tetrahedral sheets of a T–O–T layer have the structure of Figure 6b. This suggests that the arrangement of atoms at the interface shown in Figure 6a is favored over that of Figure 6b. The number of layers examined here is, of course, too small to draw a general conclusion on the energetically most favorable atom configuration at the interface.

The actual tetrahedra near the interface may be reorganized to minimize the configuration energy, presumably by the incorporation of some foreign atoms or vacancies in octahedral layers. The continuous 10Å lattice fringe images across the interface suggest that the displacement of the T–O–T layers by one-half of the *c* axis perpendicular to the layers, which occurs in the double or triple chain silicate minerals (Veblen and Burnham, 1978), may not be feasible for interfaces between muscovite and biotite.

Reorganization of the atoms near the gap regions mentioned above would not be accompanied by long-range strain fields as for misfit dislocations, since individual octahedral layers and K ion sheets are in registry in both micas. This may explain why we did not observe image contrast characteristic of dislocations at the interface.

Interfaces parallel to the mica layers

In general, the lattice parameters *a* and *b* of biotite are about 3% larger than those of muscovite. This will result in misfit on the interface when the two minerals meet epitaxially on the (001) plane. The difference in their *a* lattice parameters might be accommodated by the introduction of edge dislocations at an interval of every 30 unit cells, or 150Å. Occurrences of such dislocations are not obvious in the regions of the (001) interfaces, as shown in Figure 1. It may be that the relaxation of the strain field near the interface results in fewer misfit dislocations than expected from a simple analysis of the unit cell dimensions.

A parallel interface is represented at a higher magnification in Figure 7. The boundary between bitotite (B) and muscovite (M) is indicated by arrows. In this instance, the interface is restricted to a single (001) plane. The crystal has been aligned at the zone axis setting of biotite. The lattice fringe images of the basic 10Å layer have not been imaged in most parts of the muscovite, but fringes of 20Å appear. This is a typical phenomenon for lattice images formed when a crystal of muscovite is in a slight off-zone axis setting. In other words, the crystal orientations of the two minerals are not exactly coincident. It is not clear whether such a slight misorientation between the two micas results from the difference between their lattice parameters.

Splits of the fringe images indicated by arrows pointing down are a secondary effect that takes place under the electron beam during observation.

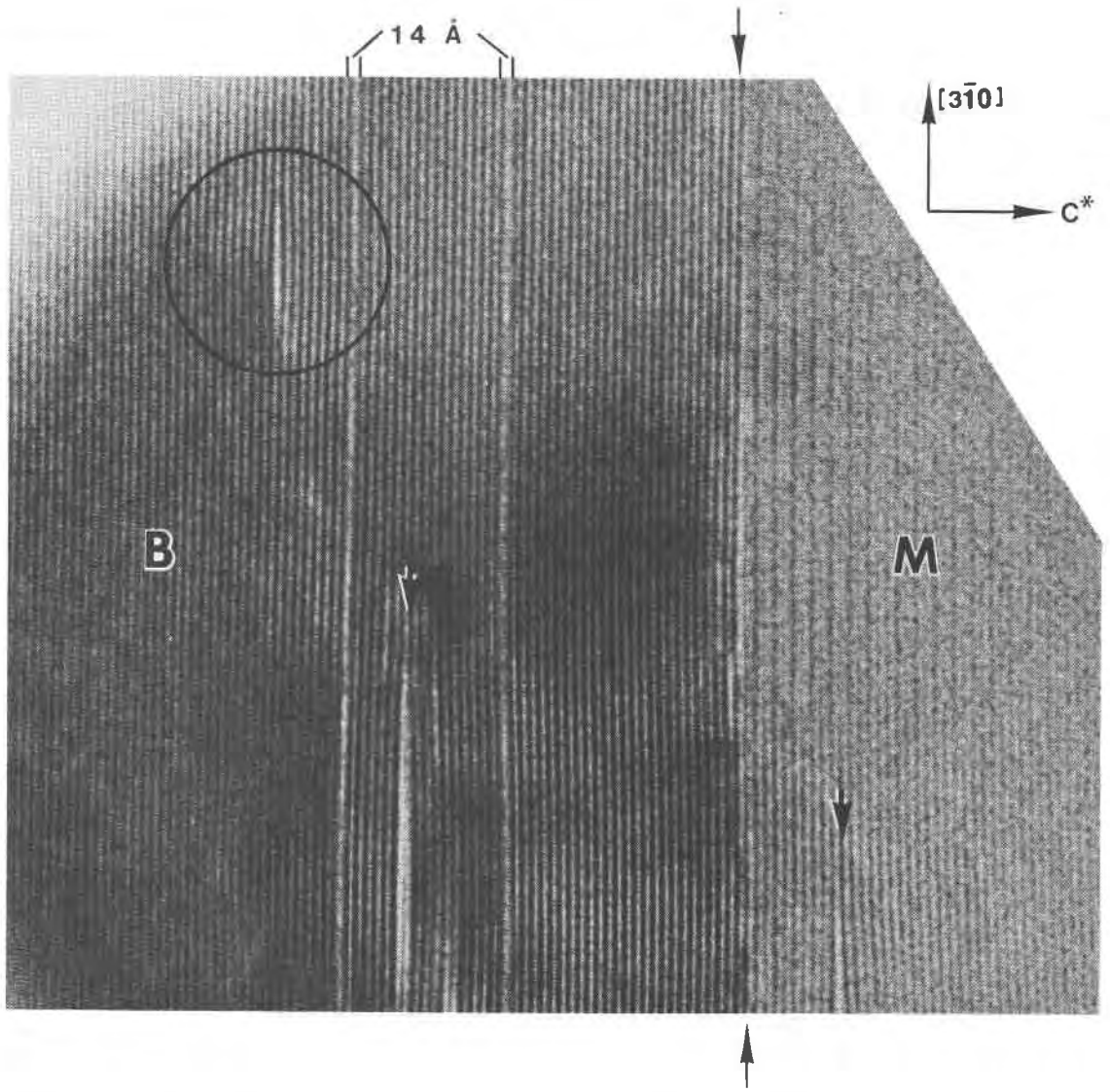

Fig. 7. A high resolution lattice image showing a region of the muscovite–biotite interface (arrowed) which is parallel to the basal (001) plane. Two slabs having a spacing 14Å are indicated and could be explained as intergrowths of single layers of chlorite-type structure. Such intergrowth occurs frequently near the parallel interface. The convex lens shapes are the initial stages of splitting of the mica layers, which results from mechanical stress during the specimen preparation.

Such specimen damage will be discussed in the section, "Damage due to electron beam irradiation."

Intergrowth of chlorite-type layers

In the biotite region shown in Figure 7 there are two vertical lines having lighter contrast than those in the rest of the area. The widths of these narrow bands were measured to be about 14Å (the distance between the two adjacent dark lines). They occur always as isolated single bands. It is likely, therefore, that the K ion interlayers are replaced with slabs wider than that of the K ion interlayer of mica.

A possible layer would be a single layer of brucite $Mg(OH)_2$, which would satisfy the 14Å spacing and produce a single unit cell of chlorite. Since the primary difference between mica and chlorite is in the interlayer, these two minerals can be intergrown coherently. In fact, such a coherent intergrowth has been found in phyllosilicate by Page and Wenk (1979) and also Veblen and Buseck (1981).

The chlorite-type intergrowth layers occur al-

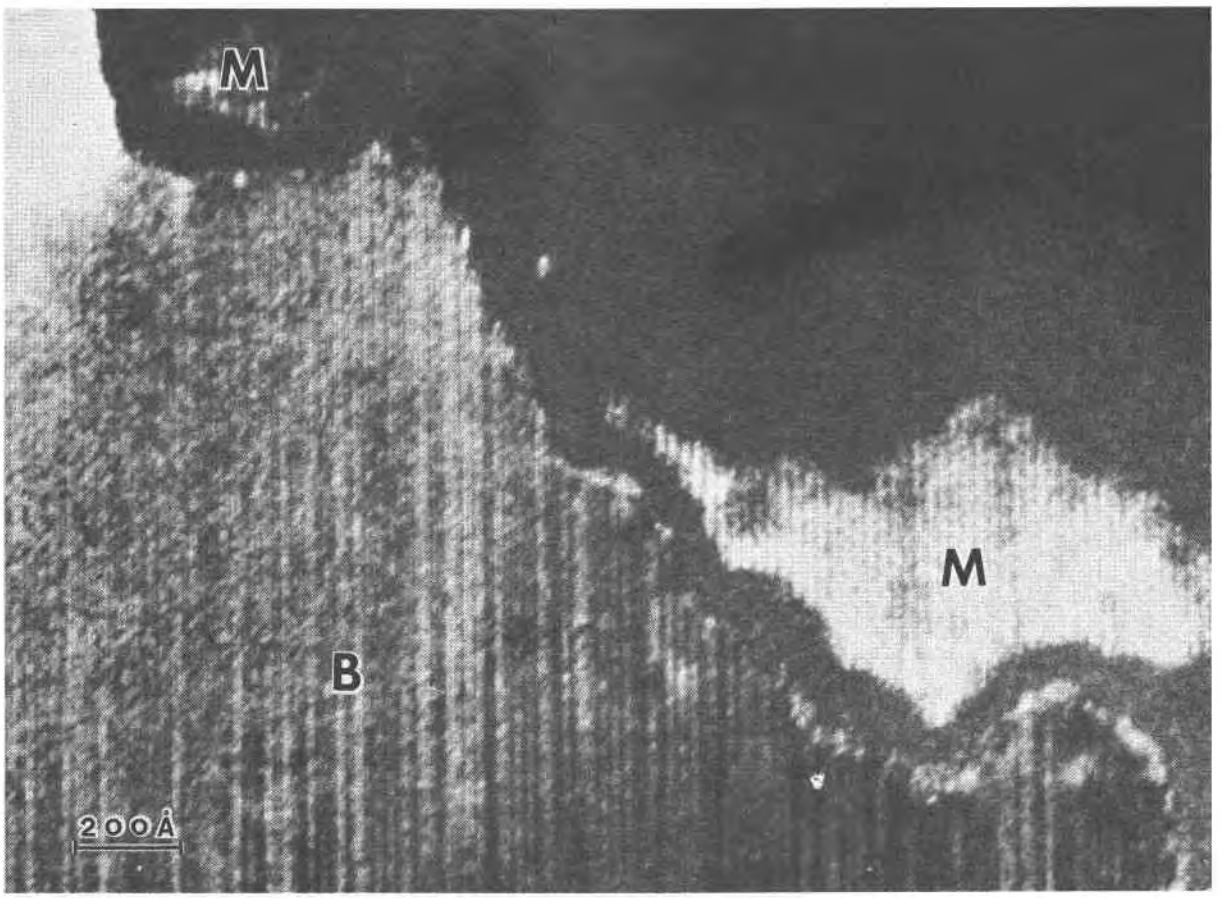

Fig. 8. A dark field image of a region corresponding to the area enclosed by the large rectangle of Fig. 3, showing the effect of electron beam irradiation. Some parts of the muscovite have been vitrified due to the beam damage. The dark regions between muscovite and biotite where the vitrification has been completed indicate that the interface was a nucleation site for the vitrification.

ways as isolated single slabs and are observed only in the vicinity of the biotite–muscovite interface. Two possible reasons for the chlorite-type intergrowths in biotite are as follows: (1) The intergrowth is associated with the lattice strain at the interface, which has been accommodated by the occasional intergrowth of chlorite-type layers, since they have smaller *a* and *b* lattice dimensions than those of muscovite. In going away from the interface, the misfit at the interface can be relaxed more rapidly by having chlorite-type structure. This would explain why there are not chlorite-type layers in regions very far from the interface. (2) Their occurrence could be associated with a composition variation of the biotite or could result from diffusion processes in the history of the mica book. Diffusion of the Mg ions, combined with deficiency of the K ions, would be of importance in producing the layers.

In place of edge dislocations, the occurrence of which has been proposed by Gresens and Stensrud (1971) in order to accommodate the difference in the *c* lattice parameters between muscovite and biotite, the chlorite-type layers could absorb the interface misfit. It is noted that the *c* axis of biotite is larger than that of muscovite, so that the intergrowth of chlorite in biotite would have the same effect as edge dislocations in muscovite.

Damage due to electron beam irradiation

In our ample experience with examining various silicate minerals under the electron microscope, it has generally been true that resistance of the materials to electron beam irradiation depends on amount of OH ions present. For instance, chlorite is less stable than micas. Similarly, clay minerals containing much more water are rapidly damaged by the beam.

It was found in the present study that biotite is much more stable in the electron beam than muscovite. This is demonstrated in Figure 8, which corresponds to a region enclosed by the large rectangle in Figure 3. The micrograph is a dark field image taken under the same conditions as that of Figure 4b. Two regions marked M are muscovite, but the rest of the original crystal of muscovite has been vitrified. It is noted that the vitrification of muscovite nucleates along the interface. This can be recognized in Figure 8 by the enhanced vitrification between remaining muscovite and biotite. Nucleation at the interface is quite reasonable because the damage could start at gap regions at the boundaries.

The reason for the instability of muscovite may lie in the chemistry of the octahedral layers. Biotite is richer in Fe ions than muscovite and is commonly richer in F and poorer in OH ions; therefore it is more resistant. It is also possible to explain differences of behaviour of biotite and muscovite under the beam due to slightly higher ionization energy for Fe ions than Al ions.

A feature with a convex lens shape similar to an intrinsic stacking fault is circled in Figure 7. This is an image showing the initial stage of splitting of the crystal (indicated by larger arrows), which is a common phenomenon due to mechanical stress during specimen preparation. We can not tell convincingly from this image where the split starts. However, the split may have occurred at the K ion interlayers because the T–O–T sheets are strongly bonded. If we assume so, then the dark lines in the region of biotite would correspond to the T–O–T layers. This allows us to tell that the intergrowth layer of 14Å width results from replacing the K ion layer by the $Mg(OH)_2$ layer as mentioned in the preceding section.

Conclusion

Atomic arrangements of the interface of coexisting muscovite and biotite in a mica book from Mitchell Creek Mine, Georgia, have been inferred using the high resolution transmission electron microscope.

The crystallographic morphologies of the interface obtained by light microscope observation are merely averaged structures (Gresens and Stensrud, 1971). The electron microscope shows that the interface is more complex. In the extreme case, a narrow band of muscovite 300Å wide penetrates into a biotite region.

The muscovite of the mica book examined in the present study has a well ordered $2M_1$ polytype structure, while the biotite is considerably disordered. The individual octahedral sheets were found to be continuously connected from biotite to muscovite at their interface. Discontinuity, however, occurs in the tetrahedral sheets. There are only two possible atomic arrangements for the discontinuity, if the boundary is sharp, and one of them seems to be energetically more favorable than the other.

Single layers of chlorite-like structure are commonly intergrown in biotite near the (001) interfaces. This intergrowth might promote relaxation of the lattice strain produced by the contrast of the two micas or might result from diffusion processes involving the Mg ions in the present mineral system.

Biotite is more resistant to electron beam irradiation than muscovite, which may be attributed to its being poorer in OH ions. The electron beam damage of the specimen initiates at the interface. This may be caused by dislocations at the interface.

Acknowledgments

We would like to thank Dr. N. Guven of Texas Tech. University for providing the mica specimen and Dr. D. Veblen for improving the manuscript. We thank Mr. H. Kolar for his help in the X-ray micro-analysis. Financial support from NSF Grant DMR-8015785 is gratefully acknowledged. This research was also supported by the NSF HREM facility at ASU (Grant CHE-7916098).

References

Gresens, R. L. and Stensrud, H. L. (1971) Chemical, optical, and x-ray analysis of an unusual muscovite–biotite intergrowth. Lithos, 4, 63–69.

Iijima, S. and Buseck, P. R. (1978) Experimental study of disordered mica structures by high-resolution electron microscopy. Acta Crystallographica, A34, 709–719.

Iijima, S. (1982a) High-resolution electron microscopy of mcGillite: I. Structure determination. Acta Crystallographica, 38A, 685–694.

Iijima, S. (1982b) High-resolution electron microscopy of mcGillite: II. Polytypism and disorder. Acta Crystallographica, 38A, 694–702.

Lester, J. G. (1946) Inclusion in muscovite from Mitchell Creek Mine, Upson County, Georgia. American Mineralogist, 31, 77–81.

Page, R. and Wenk, H. R. (1979) Phyllosilicate alteration of plagioclase studied by transmission electron microscopy. Geology, 7, 393–397.

Ross, M., Takeda, H. and Wones, D. R. (1966) Mica polytypes: systematic description and identification. Science, 151, 191–193.

Smith, J. V. and Yoder, H. S. (1956) Experimental and theoretical studies of the mica polymorphs. Mineralogical Magazine, 31, 209–235.

Veblen, D. R. and Buseck, P. R. (1981) Hydrous pyriboles and

sheet silicates in pyroxenes and uralites: Intergrowth microstructures and reaction mechanisms. American Mineralogist, 66, 1107–1134.

Veblen, D. R. and Burnham, C. W. (1978) New biopyriboles from Chester, Vermont: II. The crystal chemistry of jimthompsonite, clinojimthompsonite, and chesterite and the amphibole–mica reaction. American Mineralogist, 63, 1053–1073.

Zvyagin, B. B. (1962) The theory of mica polymorphism. Soviet Physics Crystallography, 6, 571–580.

Manuscript received, January 5, 1982;
accepted for publication, June 21, 1982.